PAPER • OPEN ACCESS

Irregular macroscopic dynamics due to chimera states in small-world networks of pulse-coupled oscillators

To cite this article: A Rothkegel and K Lehnertz 2014 *New J. Phys.* **16** 055006

New Journal of Physics
The open access journal at the forefront of physics
Deutsche Physikalische Gesellschaft DPG | IOP Institute of Physics

Irregular macroscopic dynamics due to chimera states in small-world networks of pulse-coupled oscillators

A Rothkegel and K Lehnertz

Department of Epileptology, University of Bonn, Germany
Helmholtz Institute for Radiation and Nuclear Physics, University of Bonn, Germany
Interdisciplinary Center for Complex Systems, University of Bonn, Germany
E-mail: Alex.Rothkegel@web.de

Received 17 December 2013, revised 3 March 2014
Accepted for publication 11 March 2014
Published 7 May 2014

New Journal of Physics **16** (2014) 055006

doi:10.1088/1367-2630/16/5/055006

Abstract

We study the collective dynamics of excitatory integrate-and-fire-like oscillators interacting via δ-pulses on a small-world network. The oscillators are endowed with refractory periods and time delays. For weak coupling strengths, the network self-organizes into synchronous and asynchronous regions. Such chimera states allow for two separate routes to synchrony/asynchrony. In addition to the loss of stability of either synchronous or asynchronous regions mediated by long-ranged connections, regions may grow or shrink mediated by the lattice structure. The interplay between these behaviors leads to controlled total sizes of asynchronous regions or to an alternation of synchronization and desynchronization phenomena with irregular macroscopic observables.

Keywords: small-world network, synchronization, chimera states, brain

1. Introduction

Synchronization phenomena in complex networks of interacting oscillatory systems have been studied in many different contexts in natural and life sciences [1–6]. Examples from

physiology include pacemaker cells in the heart [7], insulin-secreting cells in the pancreas [8], neuron networks in the brain [9–13], and interactions between such systems [14, 15]. Lacking the ability to simultaneously acquire the dynamics of the system's constituents, modelling studies are conducted in which the emergence of either (partially) synchronous and asynchronous states is related to the structural properties of the network and its constituents. In a network that comprises a lattice structure, the dynamical behaviors can become uncorrelated for distant oscillators, as, for example, in so-called *chimera states*, in which oscillators split into two domains, one of which is synchronized and phase-locked while the other is asynchronous [16–24]. Chimera states are usually studied in lattices of identical oscillators and have been met with surprise by the community as they present a form of symmetry breaking: the equations of motions are translation invariant, while the chimera state is not. A common observation that can be made in large complex systems is that macroscopic observables are a lot more regular than microscopic ones. This is well reflected by many of the mentioned synchronization phenomena: for large systems they lead to either constant or periodic macroscopic dynamics. However, there are exceptions to this rule in which fluctuations and irregular behavior extend from the microscopic to the macroscopic scale. A prominent example is the brain, which shows irregular global activities both for physiological and pathophysiological functioning.

In an earlier study [25], we reported on irregular macroscopic dynamics in small-world networks of pulse-coupled oscillators. Specifically, these network are capable of generating recurrent events of synchrony, which could occur either periodically in the form of a network-generated rhythm or irregularly and separated by long and seemingly stationary periods of asynchronous behavior. We here extend upon this study and relate the generation of these macroscopic dynamics to chimera states, which allow for different kinds of entrainment to either the synchronous or the asynchronous part of the network, reflecting dual structure: entrainment can be mediated by either the short- or the long-ranged connections leading to growing or shrinking of asynchronous regions, or to a loss of stability of either asynchronous or synchronous regions. The excitations that are distributed over the network via long-ranged connections can be considered as a mean field which—depending on the spatial pattern of oscillator phases—may allow or prevent each of these four possibilities. Due to this self-generated mean field, the oscillators in the networks organize into chimera states with either stable total sizes of asynchronous regions or with irregular sizes. In the latter case, synchronization and desynchronization phenomena alternate, leading to irregular macroscopic network dynamics.

This paper is organized as follows. In section 2 we present our oscillator model and provide an overview of its dynamical behaviors, which includes irregular macroscopic dynamics. In section 3, we discuss the generation of chimera states for control parameters for which the separation into synchronous and asynchronous regions is stable and immobile once assumed. In section 4, we explain the mechanisms that underlie the evolution of spatial patterns in chimera states, thereby regarding small-world networks as lattices subject to a self-generated forcing. In section 5, we describe the different kinds of irregular macroscopic dynamics and show how these mechanisms lead to their generation. Finally, in the conclusion section (section 6) we summarize our findings and relate them to prominent observable dynamics in the brain.

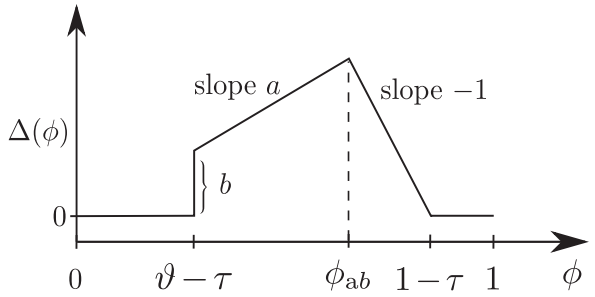

Figure 1. Schematic for the phase response curve $\Delta(\phi)$ as given in (2).

2. The Model

We study a network of oscillators $n \in N$ with cyclic phases $\phi_n(t) \in [0, 1)$ and intrinsic dynamics $\dot{\phi}_n(t) = 1$. If for some t_f and some oscillator n the phase reaches 1, the oscillator fires and we introduce a phase jump in all oscillators n' that are connected to n according to some network. The height of the phase response is defined by the phase response curve $\Delta(\phi)$:

$$\phi_{n'}\left(t_f^+\right) = \phi_{n'}\left(t_f\right) + \Delta\left(\phi_{n'}\left(t_f\right)\right). \tag{1}$$

For $\Delta(\phi)$ we choose a piecewise linear form (see figure 1)

$$\Delta_{\tau,\vartheta}(\phi) = \begin{cases} 0 & 0 < \phi \leqslant \vartheta - \tau, \\ a(\phi - \vartheta + \tau) + b & \vartheta - \tau < \phi \leqslant \phi_{ab}, \\ 1 - \tau - \phi & \phi_{ab} < \phi \leqslant 1 - \tau, \\ 0 & 1 - \tau < \phi \leqslant 1, \end{cases} \tag{2}$$

where $\phi_{ab} = \frac{1-b-\vartheta}{a+1} + \vartheta - \tau$. The PRC represents an integrate-and-fire (IF) oscillator [26, 27] endowed with refractory periods ϑ and time delay τ. The phase variable was shifted in order to obtain formally undelayed oscillators and to incorporate τ directly into the PRC; the firing of the oscillator corresponds to a phase of $\phi = 1 - \tau$, while its excitations are received by connected oscillators when $\phi = 0$. Note that such an interpretation is only possible for identical time delays $\tau < \vartheta$ on all outgoing connections of an oscillator and for oscillators that are refractory between firing and the receipt of their excitation by another oscillator. Excitations are limited to the firing threshold such that for suprathreshold excitations, oscillators are left with a phase of $1 - \tau$ (see the third case of (2)). The excitable state of oscillators is represented by the second case of (2), where we assume a linear dependence on ϕ. Such oscillators behave very similarly to standard IF oscillators. The parameter b can be thought to control the coupling strength of oscillators, and a controls both the coupling strength and the leakiness. Many dynamical behaviors do not depend largely on the exact form of the PRC in the excitable state [27]. Compared to our earlier study [25], we choose the simpler phase response curve here.

As a network topology we start with a square arrangement of nodes, in which every node is connected bidirectionally to its m nearest neighbors. In the case where m does not define a unique set of neighbors, we choose randomly between nodes with the same distance. We use cyclic boundary conditions such that the lattice forms a torus. We then remove a certain fraction

ρ of directed connections and introduce the same number of connections between randomly chosen source and target nodes [28]. The newly introduced connections will, with large probability, connect nodes with a large distance on the lattice. Varying the fraction ρ of such long-ranged connections between 0 and 1 allows to us to interpolate continuously between regular lattices and directed random networks while keeping the total number of connections in the network fixed. The archetypical behavior of dynamical systems coupled onto lattices are waves [29], while for random networks synchronization phenomena are often studied [30]. Both behaviors can be expected to be carried over to the small-world regime ($0 < \rho < 1$), which allows us to study the interplay of spatial patterns and global oscillations [31]. The construction scheme requires us to choose the network size N, the fraction of long-ranged connections ρ, and the number of nearest neighbors m. For large network sizes N, constructed networks with the same parameters show very similar behavior. Moreover, for larger m, we generate networks in which different nodes have similar amounts of short- and long-ranged connections and the target nodes of the replaced connections are well distributed over the network such that the incoming excitations of some oscillators can be considered as a sampling of the mean firing rate. We can thus regard the constructed networks as a medium in which the mean firing rate is coupled to each site.

In dependence on control parameters, the networks show a large spectrum of dynamical behaviors that are crucially influenced by the formation of spatial patterns. Unless specified otherwise, we fix the oscillator parameters as $\tau = 0.01$, $\vartheta = 0.05$, and choose $a = b/2$. The height of the phase responses is thus controlled by parameter b only. Moreover, we choose $m = 50$ connections per oscillator, and we usually choose uniformly distributed phases as the initial conditions. To characterize the macroscopic dynamics, we assess the order parameter $r(t) = 1/N \sum_{n \in N} e^{i\phi_n(t)}$ and the firing rate $\nu(t)$ and relate the global behavior to patterns in the spatial distribution of oscillator phases, in dependence on ρ and b. Numerical simulations were performed with Conedy [32], which uses event-driven algorithms to integrate the dynamics.

Macroscopically, we observe asynchronous states with nearly constant firing rates $\nu(t)$ and synchronous states with periodic time evolutions of $\nu(t)$. Both can co-occur with different spatial patterns. For the small values of τ and ϑ we are considering here, wave phenomena are fast compared to the intrinsic frequency of oscillators, and wave-dominated states are possible in which oscillators mostly fire because they are excited and not because of their intrinsic dynamics. The dynamics of the wave-dominated states then is similar to what can be observed for excitatory IF neurons [33]. Additionally, we observe a regime in which macroscopic observables are irregular and show no convergence to either constant or simple periodic behavior, contradicting the classical notion of synchronous and asynchronous states. In this regime, $r(t)$ exhibits small amplitude oscillations, which reflect the average phase velocity of oscillators. However, these oscillations range around values that themselves may exhibit complicated time evolutions. The network behavior can take the form of short periods of synchronous firing embedded into long periods of asynchronous behavior (see figure 2, top left) or of an oscillatory rhythm that is several times slower than the eigenfrequency of oscillators (see figure 2, top right). Moreover, we observe evolutions in which synchronization and desynchronization phenomena alternate in an irregular manner (see figure 2, bottom). To detect non-converging behavior, we calculate the sequence of local maxima $\hat{r}(t)$ of $r(t)$ in which the influence of the small amplitude oscillations is eliminated. Both asynchronous states and synchronous states will lead to constant values of $\hat{r}(t)$, while more complicated time evolutions

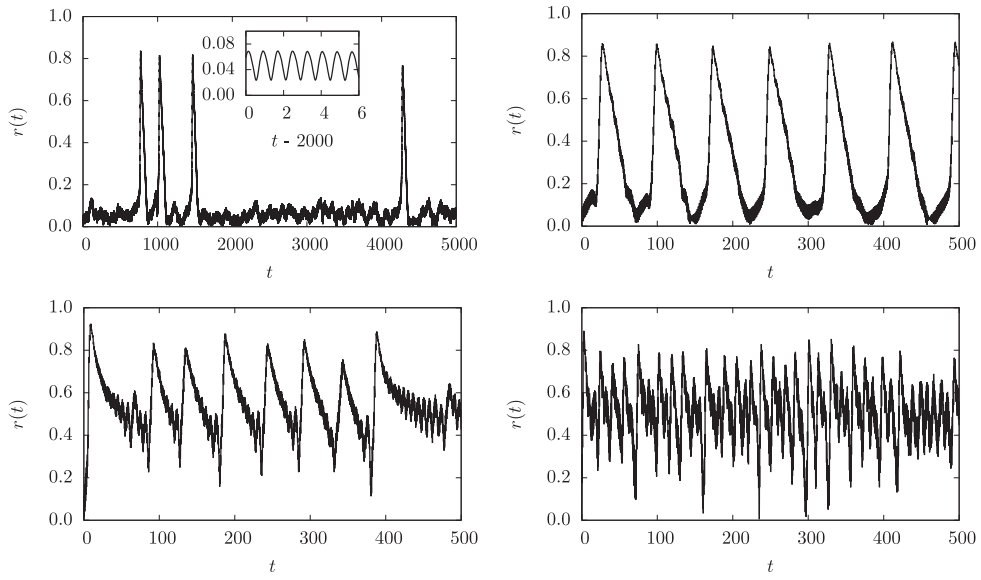

Figure 2. Time evolution of the order parameter $r(t)$ of small-world networks $(N = 250 \times 250)$ of IF oscillators. Initial condition: uniformly distributed phases. Top left: $(\rho, b) = (0.56, 0.004)$; top right: $(\rho, b) = (0.54, 0.006)$; bottom left: $(\rho, b) = (0.56, 0.008)$; bottom right: $(\rho, b) = (0.48, 0.0012)$. The top left plot shows a closer view, revealing small amplitude oscillations that are present in all four time evolutions.

can be assessed by the statistical properties of $\hat{r}(t)$ that characterize fluctuations. While the mean of $\hat{r}(t)$ provides similar information to the mean of $r(t)$ itself, the range of assumed values reveals around $\rho = 0.5$ the mentioned region with non-converging network activity. For investigated network sizes up to $N = 750 \times 750$, the fluctuations in $\hat{r}(t)$ did not decrease with N, nor did the size of the region in parameter space for which networks exhibit this behavior. We therefore assume that the behavior is not a consequence of finite-size effects. A visual inspection of the statistical properties of $\hat{r}(t)$ and $\nu(t)$ (upper and middle parts of figure 3) allows us to distinguish different regions in parameter space spanned by b and ρ that differ in the dynamical behavior (figure 3, bottom). An investigation of the divergence of trajectories allows us to classify the dynamical behaviors as chaotic, with the exception of the synchronized and phase-locked states for large and small values of ρ, respectively. The wave dominated states that can be observed for larger values of b are comparable to those we described for a similar dynamical system [33], and we therefore refrain from a detailed description. Instead, here we discuss the non-converging behavior that can be observed in regime IIIb as defined in figure 3. Note that the dynamical behaviors in regimes V and IIIb most likely do not correspond to attractors but rather have to be considered as complicated transients to synchrony. Both can only be observed for larger network sizes, while smaller sizes lead to synchrony after a transient of variable duration. With increasing system size (large N), the mean transient duration grows exponentially, making the attractor unobservable and the transient the generic dynamical behavior, similar to e.g. turbulence in fluids [34]. For large random networks, a sharp transition between long transients and short transients is established in dependence on the control parameter b. The long transients consist of seemingly stationary, asynchronous behavior and

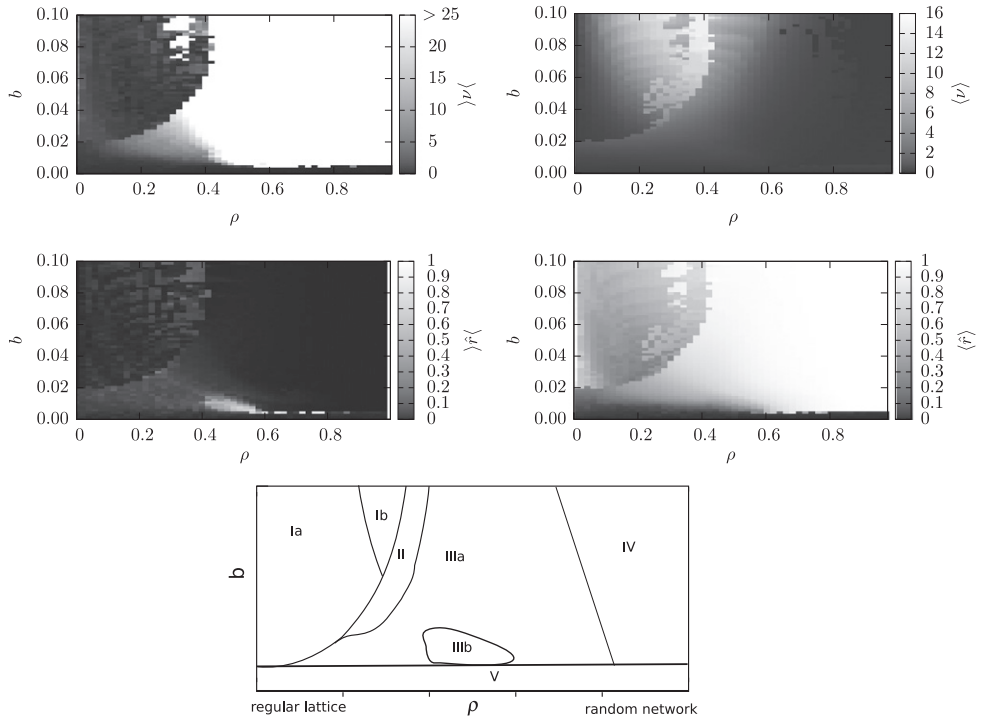

Figure 3. Statistical properties of the firing rate $\nu(t)$ and of the local maxima $\hat{r}(t)$ of the order parameter for small-world networks ($N = 250 \times 250$) of IF oscillators in dependence on the fraction of long-ranged connections ρ and the oscillator parameter b. Initial condition: uniformly distributed phases. Top left: range $\rangle\nu\langle := \max(\nu) - \min(\nu)$ of observed values of $\nu(t)$; top right: average $\langle\nu\rangle$ of $\nu(t)$; bottom left: range $\rangle\hat{r}\langle$ of $\hat{r}(t)$; bottom right: average $\langle\hat{r}\rangle$ of $\hat{r}(t)$. Values were obtained for $t \in [100, 200]$. Bottom: schematic of the parameter regimes as distinguished by spatial patterns and macroscopic dynamics. Ia: cyclic waves without global synchrony. Ib: cyclic waves with global synchrony. II: spiral waves without global synchrony. IIIa: networks split into synchronous regions and asynchronous regions that are unstructured for smaller phase responses and which take the form of turbulent-like waves for larger ones. The relative sizes of synchronous and asynchronous regions is fixed. IIIb: networks split into synchronous and unstructured asynchronous regions that fluctuate in both size and shape. IV: almost completely synchronized state in which all excitations are received during the refractory period of oscillators. V: asynchronous state with constant firing rate and distribution of phases.

end with the formation of a phase cluster and avalanche-like synchronization within a few collective oscillations. The different non-converging behaviors that we will report on here emerge when this transition is carried over into the small-world regime. Instead of short transients to synchrony, we observe in small-world networks chimera states, a separation into synchronous and asynchronous regions, which we will show play a crucial role in the generation of the non-converging behaviors. We therefore discuss the generation of chimera states in our networks first, for values of ρ larger than those of regime IIIb in figure 3, where the separation is stable and immobile once assumed.

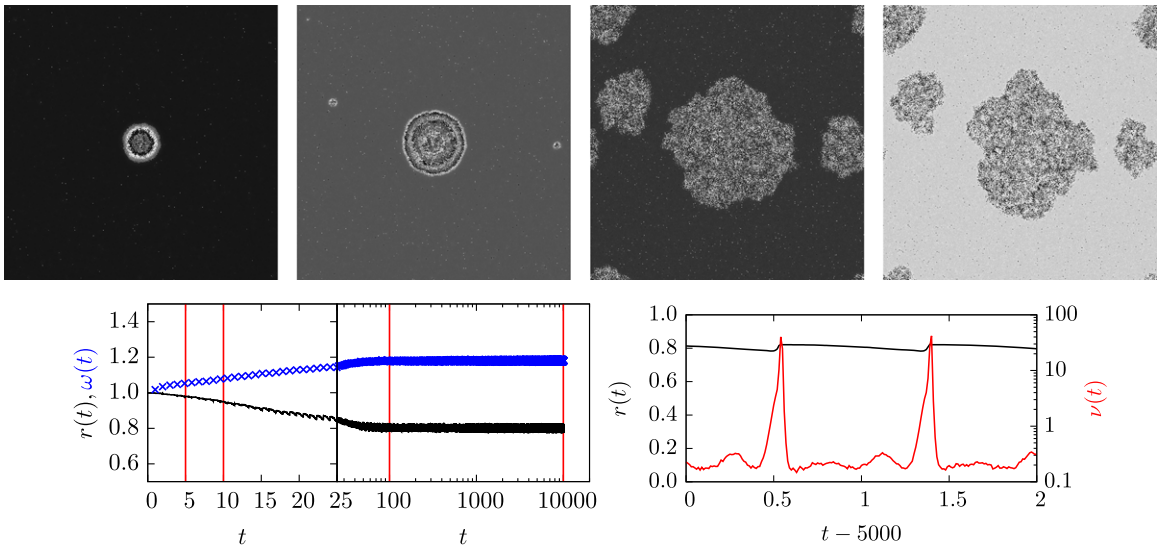

Figure 4. Snapshots of the spatial distribution of phases taken from a small-world network ($N = 500 \times 500$, $\rho = 0.64$) of IF oscillators ($b = 0.008$). Phase values range from 0 (black) to 1 (white). As an initial condition, we chose a small circle of radius 10 with uniformly distributed oscillator phases; other oscillators start with phase 0. Times of snapshots are marked as vertical lines in the bottom left plot, which shows the time evolution of the order parameter $r(t)$ and the inverse $\omega(t)$ of times between collective firings. As the small disturbance with distributed phases grows in size, other asynchronous regions are generated. When asynchronous regions reach a certain size, their shape is frozen. The different asynchronous regions do not form perfect circles, which we relate to inhomogeneities in the network structure. The bottom right plot shows a closer view on the firing rate ν and the order parameter $r(t)$ for $t \in [5000, 5002]$.

3. Chimera states

For $\rho > 0.6$ and small phase responses, the small-world networks split into a partition of unstructured asynchronous regions and synchronous regions, in which the oscillators share a common phase. The partition once assumed is 'frozen', and remains almost stable, varying little over the period of a few thousand collective oscillations. In contrast to chimera states that have been observed in lattices, those observed in the small-world networks have a stable total size of asynchronous regions; if we choose an initial condition with small asynchronous regions, they will grow until the stable total size is reached. Then again, the same total number of asynchronous regions is reached if we start with asynchronous regions covering the network (e.g. by choosing uniformly distributed initial phases). In figure 4, we show an evolution to a chimera state starting from a small localized region with distributed phases in an otherwise synchronous network. For the chosen parameters, the disturbance grows in size via the short-ranged connections. Moreover, excitations via long-ranged connections lead to a small jitter in the synchronized background. At times, additional disturbances may be created, which also grow in size. Intriguingly, the speed of growth is not constant but diminishes with the total size of the asynchronous regions. When a critical total size is reached, the growth stops, which leads to the frozen partition of the network.

The growing of asynchronous regions is influenced by the overall distribution of patterns, i.e. by the relative fraction of synchronous and asynchronous regions. The shape and distribution of asynchronous regions have a much smaller influence than their total size. On a much longer time scale, smaller asynchronous regions shrink and vanish in favor of larger ones. A circular arrangement of the asynchronous region minimizes its boundary surface to the synchronous region. It is plausible that such a shape is more stable; every deviation from it will create an insular that receives more excitations from the synchronous part than other regions. This insular is thus more likely to be entrained than other regions, leading back to the circular shape. Inhomogeneities in the random networks, however, may prevent the formation of a single asynchronous region.

Due to the long-ranged connections, an oscillator in the network is connected to other oscillators which are distributed randomly over the network. For larger mean degrees m, the incoming excitations (mediated by long-ranged connections) of an oscillator can thus be considered as a sampling of the mean firing rate in the network. Neighboring oscillators will be subject to different sequences of excitations that, however, have similar statistical properties. As an approximation, we can assume that every oscillator is subject to a Poisson process, which we regard as a mean field generated by excitations via long-ranged connections. For a given fraction of long-ranged connections ρ and mean degree m, this Poisson process has a rate $m\rho\nu(t)$ determined by the firing rate $\nu(t)$ in the network. To test that such a mean field is a valid description for our networks, we investigated similar small-world networks in which we chose targets for excitations every time an oscillator fires, instead of choosing fixed targets for long-ranged connections, when constructing the network. It is clear that the incoming excitations of some oscillators are described by a Poisson process for a large network of such kind, for which we observe qualitatively the same dynamical behaviors that we report on here. The firing rate $\nu(t)$ of a network in a chimera state (see figure 4, bottom right) is periodic and consists of distributed firings of the oscillators in the asynchronous regions and a collective firing originating from the synchronous regions. With increasing size of the asynchronous regions, the collective firing will diminish in favor of the distributed excitations. However, the frequency of the collective firing also changes (see figure 4, bottom left), which we relate to excitations from the asynchronous to the synchronous part of the network. These excitations are received when oscillators in the synchronous part are not refractory and may thus decrease the time to the next collective firing. This is in contrast to excitations that originate from and are received by oscillators in the synchronous part. As those excitations are received by refractory oscillators, they cannot increase the frequency of the collective firing. In short, the collective firing becomes weaker and more frequent, which changes the local conditions at the boundary of asynchronous regions and influences the speed and the possibility of their growth. When the asynchronous regions reach a critical size, the growth stops and we observe changes in the spatial patterns only on a much larger time scale. Note that the dynamics of the networks in the frozen states are still chaotic, although only the asynchronous regions contribute to the chaotic dynamics.

We will now investigate the dynamical behavior when the size of the synchronous part of the network is much smaller than the stable size (see figure 5). The spatial patterns during the avalanche-like synchronization are different compared to those that are generated by growing of asynchronous regions (see figure 4). During an avalanche, only those oscillators that are shortly before the firing threshold will be entrained. Due to the irregular dynamics, such oscillators are distributed all over the network, and so is the emerging synchronous part (see figure 5).

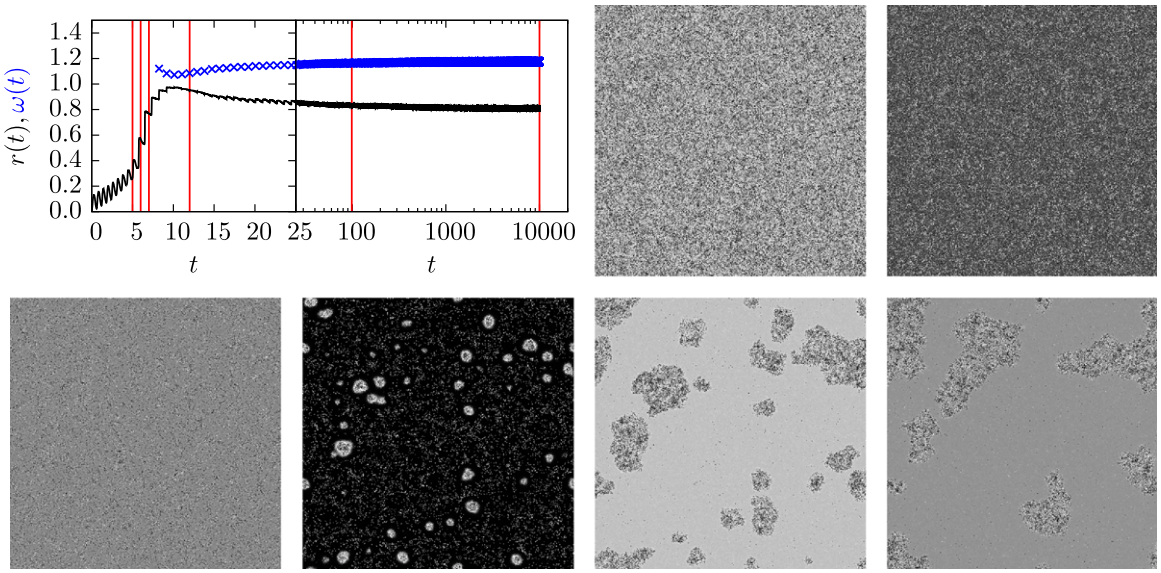

Figure 5. Snapshots of the spatial distribution of oscillator phases taken from a small-world network ($N = 500 \times 500$, $\rho = 0.64$, $m = 50$) of IF oscillators ($b = 0.008$). Phase values range from 0 (black) to 1 (white). Times of snapshots are marked as vertical, red lines in the top left plot, which show the time evolution of the order parameter $r(t)$ and the inverse $\omega(t)$ of times between collective firings. Note the change of scaling at $t = 25$. When starting from uniformly distributed phases, oscillators synchronize rapidly but not completely. A few asynchronous regions remain, which grow until they reach a critical size. Afterwards, the smaller regions shrink and vanish in favor of the larger ones until a partition of the network into synchronous and asynchronous regions is frozen.

The large *surface* between the synchronous and the asynchronous part seems to favor synchronization, as oscillators may be entrained via short-ranged and long-ranged connections; if we compare the spatial distributions of oscillator phases that have the same value of the order parameter, then $r(t)$ will decrease in time if the asynchronous regions form connected regions, and $r(t)$ will increase in time if asynchronous and synchronous regions are intertwined. This allows the order parameter to increase above the value that corresponds to the stable total size of asynchronous regions, leading to an overshoot in $r(t)$. In contrast to chaotic transients to synchrony that can be observed for random networks [35], synchronization is not complete in the small-world regime. As discussed, the size of the collective firing increases, while its frequency diminishes. At some point, the spatial-temporal chaotic dynamics becomes resistant to the collective firing. Synchronization stops when only a few asynchronous regions remain. Afterwards they grow in size, as described earlier, until the stable size of the asynchronous regions is reached and the partition is again frozen.

We claim that the incompleteness of synchronization can be understood as a resonance phenomenon. A single oscillator has an eigenfrequency of 1, and is thus best entrained by repeated excitations that arrive with a frequency of 1. However, oscillators in an asynchronous region fire with a larger *effective frequency* due to excitations via short-ranged connections and are not susceptible to entrainment by a collective firing with a frequency near 1. To test this hypothesis, we study the emerging order in a lattice that is forced by a self-generated mean field.

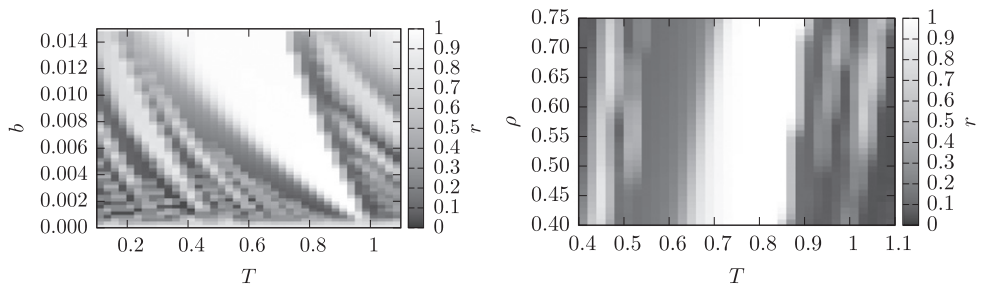

Figure 6. Average order parameter r observed in $t \in [100, 200]$ of lattices of IF oscillators subject to external forcing. Starting from a square lattice ($N = 250 \times 250$) in which each oscillator is connected to its 50 nearest neighbors, a fraction ρ of connections is removed without subsequent addition of connections. The lattices are forced by 'packets' of excitations: with temporal distance T between successive packets, $25 \cdot N$ excitations are deposited simultaneously to randomly chosen oscillators. Furthermore, every oscillator in the lattice is subject to Poissonian excitations with a rate of 12.5. Left: dependence of T and b on r for $\rho = 0.65$; right: dependence of T and ρ on r for $b = 0.005$. The large, white region in the middle of the plots is the resonance region in which oscillators synchronize 1:1 to the external forcing.

4. Small-world networks as lattices subject to a self-generated forcing

In the following, we consider a small-world network as a lattice that is forced by a self-generated mean field; we construct lattices with the same local structure as the small-world networks we are interested in. Instead of adding long-ranged connections, we introduce a forcing to each oscillator that is a simple approximation to the firing rate which we observe in small-world networks. The forcing of the lattice consists of two contributions: first, Poissonian excitations which represent excitations originating from other asynchronous regions in the small-world network, and second, concurrently arriving excitations that represent excitations from the synchronous part of the small-world network. In figure 6, we show the influence of the time T between concurrently arriving excitations on the emerging order parameter of forced lattices. As an initial condition, we chose a spatial distribution of phases that contains both synchronous and asynchronous regions. The oscillators synchronize 1:1 to the forcing for some range of values of T when the frequency of the concurrently arriving excitations is close to the effective frequency of oscillators. Moreover, we observe emerging order when these frequencies satisfy simple rational relationships, which correspond to, e.g., 2:1 synchronization. The resonance regions shift to smaller frequencies when the phase responses (controlled by b) or the number of local connections are increased. Both increments can be interpreted as strengthening of the lattice structure, which in turn increases the effective frequency of oscillators in asynchronous regions. Outside of the resonance regions, the frequencies do not match and the lattices show asynchronous behavior.

For the chimera states, we have described entrainment to the asynchronous part mediated by short-ranged connections (figure 4) and an entrainment to the synchronous part mediated by long-ranged connections (figure 5). However, for forced lattices we can also observe the other two cases of entrainment to the synchronous part via short-ranged connections and entrainment to the asynchronous part via long-ranged connections. In figure 7, we show snapshots of the spatial distribution of phases for the four cases of synchronization/desynchronization mediated

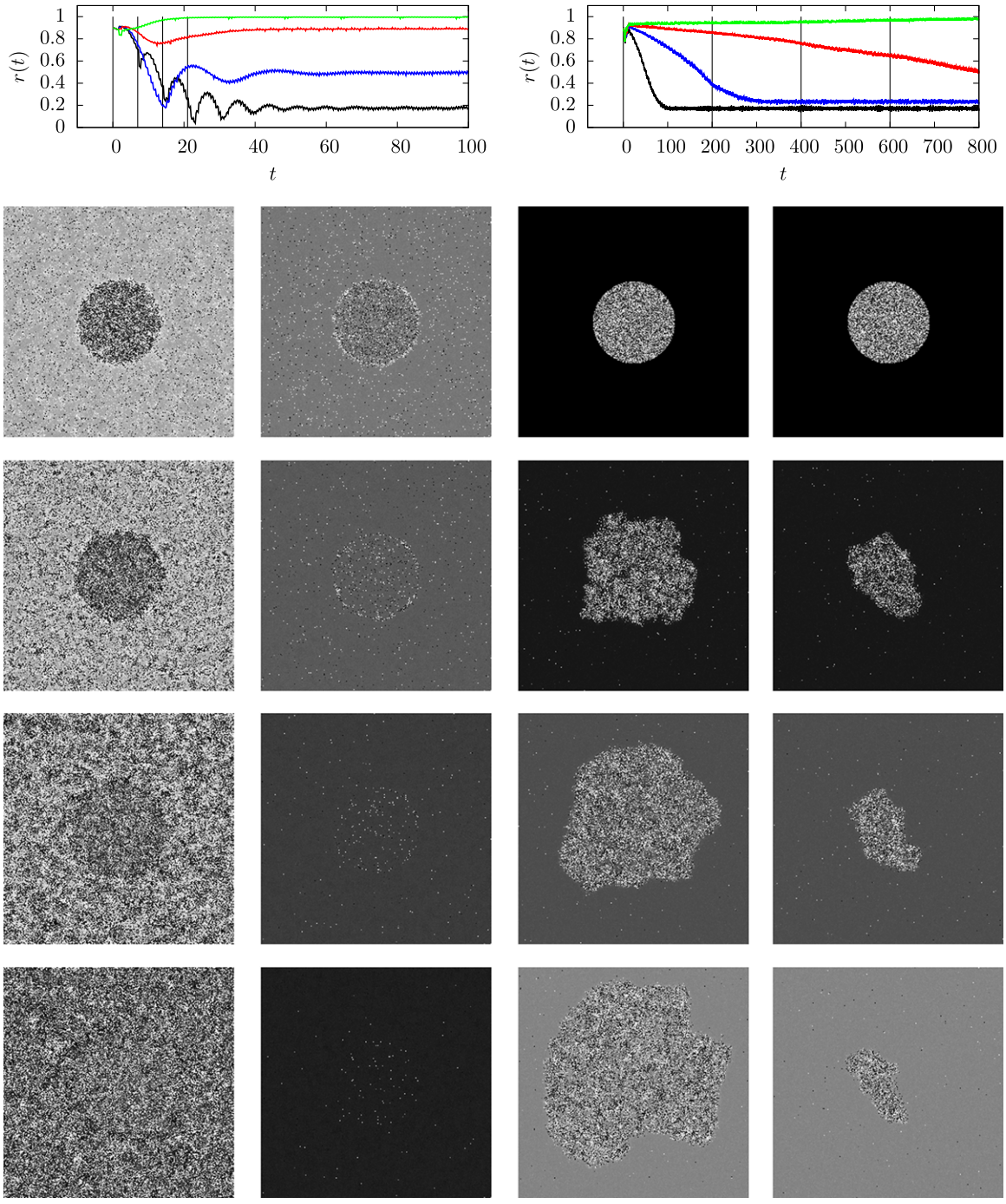

Figure 7. Exemplary time evolutions of the order parameter for forced lattices of IF oscillators (see figure 6). Left: parameter values of T to the left of the resonance region for $\rho = 0.65$, $b = 0.004$. Black: $T = 0.7$; blue: $T = 0.74$; red: $T = 0.76$; green: $T = 0.79$. Right: $b = 0.005$, $T = 0.9$, which lies to the right of the resonance region. Black: $\rho = 0.65$; blue: $\rho = 0.7$; red: $\rho = 0.72$; green: $\rho = 0.73$. Bottom: snapshots of the spatial distribution of oscillator phases taken from the black curve in the top left plot (1st column), the green curve in the top left plot (2nd column), the red curve in the top right plot (3rd column), and the green curve in the top right plot (4th column). Times of snapshots are indicated as vertical lines in the top plots.

by short-/long-ranged connections. Interestingly, we observe different behaviors for values of T that lie to the left or right of the resonance region which corresponds to 1:1 synchronization. When T is too small, the synchronous regions become unstable. At this boundary, we observe states in which the lattices do not split into chimera states. Instead, the whole lattice exhibits a homogeneous, and partially synchronous, state. The order parameter r can take any value and changes from 0.1 to near 1.0 with increasing T. To the right of the resonance region, we observe no partially synchronous states. When starting from a state that is split into synchronous and asynchronous regions, we observe either growing or shrinking of asynchronous regions. Although transients can become quite long (depending on the lattice size), the dynamics eventually settles to synchrony or asynchrony.

In small-world networks, the forcing is self-generated and depends on the relative size between the synchronous and asynchronous part (which can be related to the order parameter) and only marginally on the spatial pattern they form. We will thus write $F_r(t)$ to denote the periodic mean field that is generated for a given order parameter r. Note that the adaption of the frequency of the collective firing is related to the refractory periods that we chose for the oscillators. When the oscillators were excitable at the moment of firing, the timing of excitations would have a much smaller influence on the frequency; with increasing size of the synchronous part, the latter receives more and more self-excitations that increase the frequency just as excitations from asynchronous regions do. For the forced lattices, we described entrainment both at the border between the asynchronous and synchronous regions as well as within regions. For small-world networks and for the parameter regime we investigated, however, only synchronization within asynchronous regions and desynchronization at the border between regions seems to play a role (see figure 7, second and third column). With an eye on the non-converging behaviors that we are about to describe, we will characterize, in dependence on the spatial distribution of oscillator phases, the possibility of synchronization with set S and the possibility of desynchronization with set D.

Let us assume a distribution of oscillator phases whose asynchronous part forms regions. Such states can be characterized by the order parameter r, which basically reflects the total size of asynchronous regions. Let us consider D as those values of r, for which the mean field $F_r(t)$ generated by excitations via long-ranged connections allows for growing of asynchronous regions, and S as those values of r for which the mean field $F_r(t)$ allows for entrainment of oscillators in the asynchronous regions to the synchronous part (note that we do not measure or calculate S and D). Once entrainment of asynchronous regions (as defined in S) sets in, the distribution of patterns no longer shows a separation of synchronous and asynchronous regions such that r may increase above values that are no longer part of S. Regarding the time evolutions of the order parameter $r(t)$, we can interpret S and D graphically: S can be regarded as the set of values for which $r(t)$ begins to increase quickly to larger values, while order parameters in D allow for a steady decrease of $r(t)$. Chimera states and a stable size of asynchronous regions in the network can be related to the fact that S and D do not overlap. In figure 8, we show time evolutions of $r(t)$ starting from the initial distributions of oscillators with different values of the order parameter. The growing of asynchronous regions stops before asynchronous regions lose stability, and the dynamics of the small-world networks is therefore 'trapped' at the smallest value of r for which the growing of asynchronous regions is possible. For the parameters in the right plot, a chimera state co-exists with states in which asynchronous behavior covers the whole network.

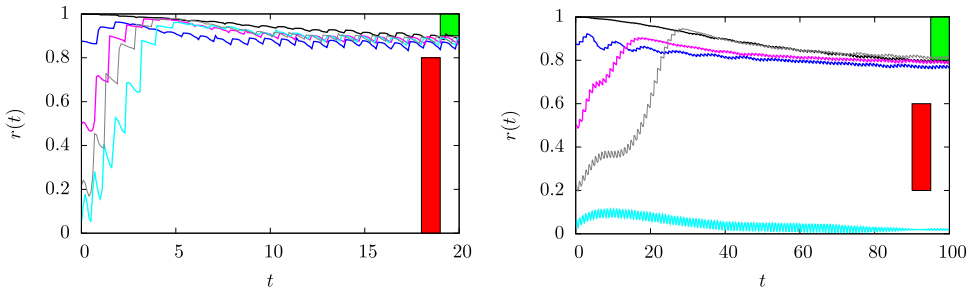

Figure 8. Time evolution of the order parameter $r(t)$ for small-world networks ($N = 500 \times 500$, $\rho = 0.65$) of IF oscillators. Other oscillator parameters were $a = 0.005$, $b = 0.01$ for the left and $a = 0.00175$, $b = 0.0035$ for the right plot. Initial condition: uniformly distributed phases for all oscillators within a distance R of some chosen oscillator, $\phi = 1$ for other oscillators. Different radii R were chosen for the circular, asynchronous region: black: $R = 10$; dark blue: $R = 100$; magenta: $R = 200$; gray: $R = 250$; light blue: $R = 300$. The red and green bars sketch the sets S and D, respectively. As both bars do not overlap, we can observe chimera states for both parameter choices of the left and right plot. For the right plot, asynchronous states are also stable.

Both types of evolution to the chimera state—that start from asynchronous regions which are either smaller or larger than the stable total size—rely on a different mechanism and are mediated by different connections within the networks. The growing of asynchronous regions is a boundary surface effect between the different regions and relies on the short-ranged connections. Synchronization of asynchronous regions from within, on the other hand, relies on long-ranged connections. By changing the fraction of long-ranged connections, we can thus expect to control the contribution of both mechanisms. It is conceivable that we can, for a given partition into synchronous and asynchronous regions, choose control parameters such that only one or both mechanisms are possible. Moreover, it seems conceivable that the growing of asynchronous regions does not stop but continues until the network is again susceptible to the forcing of the mean field that is created by the long-ranged connections, which means that sets S and D overlap. This is what happens in the small region with non-converging behavior, which we describe next.

5. Non-converging behavior

Compared to the chimera states, we observe non-converging behavior at smaller fractions ρ of long-ranged connections for which asynchronous regions are growing until synchronization may set in, leading to a constant interplay between synchronization and desynchronization. In the following, we will discuss the dynamics, traversing the region with non-converging behavior in the direction of increasing b (see figure 3). For $b < 0.004$, small-world networks exhibit asynchronous behavior, which is, for assessable observation times, stable; transients starting from a distribution of synchronous and asynchronous regions show growth in the asynchronous regions until they cover the whole network. Regarding our definitions, S is empty, while D covers nearly the whole unit interval. For $b \in [0.004, 0.006]$, the asynchronous behavior loses stability and its lifetimes assume values that allow us to observe synchronization.

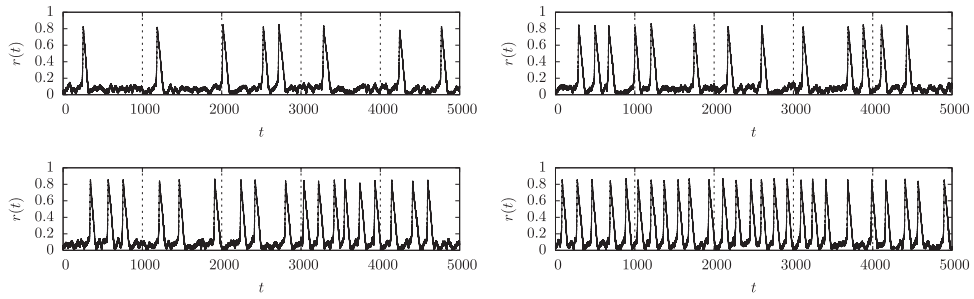

Figure 9. Time evolutions of the order parameter $r(t)$ indicating rare events of synchronous firing for small-world networks ($N = 250 \times 250$, $\rho = 0.56$) of IF oscillators for different values of b. Initial condition: uniformly distributed initial phases. From top left to bottom right: $b = 0.0042$, $b = 0.0044$, $b = 0.0046$, and $b = 0.0048$. For the chosen parameters, D contains the whole unit interval. Synchronization is not possible, and S is arguably empty. However, the asynchronous states are unstable and synchronize spontaneously with a small probability.

The networks show long periods of asynchronous behavior before a phase cluster is formed and the oscillators spontaneously start to synchronize. The initiation of synchronization is similar to chaotic transients, leading to complete synchrony, which can be observed for random networks [35, 36]. For small-world networks, synchronization is not complete but stops when the network exhibits only a few small asynchronous regions embedded in a synchronized background. These asynchronous regions grow until they cover the whole network, and the dynamics reenters the quasi-stable asynchronous state. The dynamical behavior can be described as short, spontaneously generated events of synchrony that are embedded into extended periods of asynchronous behavior. In figure 9, we show exemplary time evolutions of the order parameter. For larger network sizes, the macroscopic observables show very similar progressions during events. However, the spatial patterns that are formed by the oscillator phases are different for each event. With increasing b, the frequency of events increases (see figure 9) as the escape from the quasi-stable asynchronous state becomes easier. The dynamics during events, however, is nearly unaffected. The fraction of long-ranged connections has an influence on the duration of events (see figure 10); with less short-ranged connections, the growing of asynchronous regions becomes slower and eventually stops. At this point, the event is turned into a transient to a chimera state, similar to that presented in figure 5.

For an investigation of the statistical properties of the events, we used control parameters for which the characteristic behavior is generated by smaller networks, without being masked by finite-sized effects (see figure 11). As a further simplification of the model, we chose non-leaky oscillators ($a = 0$). The measured durations T_A between events are consistent with an exponential distribution (see figure 11, top left). Moreover, we find no correlation between subsequent durations between events (see figure 11, bottom left). The events are thus distributed in time similarly to those generated by a Poisson process. This means that the probability for an event to occur is constant during the time the networks show asynchronous behavior. This can be regarded as an indication that events are difficult to predict. The events themselves show a duration T_E that is characteristic and varies little (see figure 11, top right).

With increasing b, the mean duration between events decreases (see figure 9), until the events immediately start as soon as the whole network is covered with asynchronous regions. For

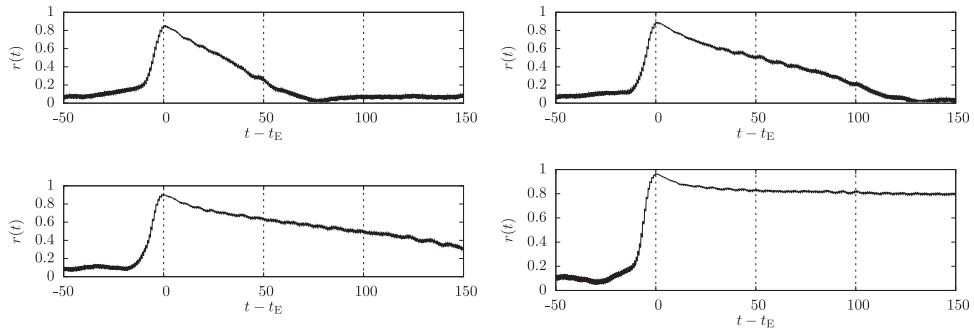

Figure 10. Time evolutions of the order parameter $r(t)$ for small-world networks ($N = 250 \times 250$) of IF oscillators ($b = 0.0045$) and for different fractions of long-ranged connections ρ. From top left to bottom right: $\rho = 0.55$, $\rho = 0.57$, $\rho = 0.59$, and $\rho = 0.64$. $r(t)$ shows an event that is aligned such that the maximum value of $r(t)$ lies at $t = 0$. With increasing ρ, the growing of the asynchronous regions slows down and eventually stops, leading to a chimera state.

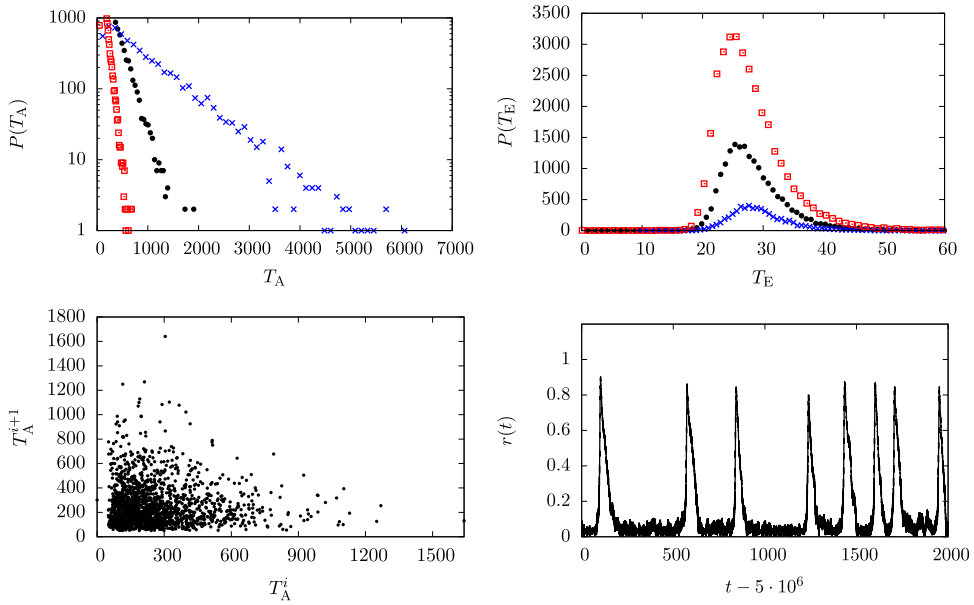

Figure 11. Top left: frequency distribution $P\left(T_{\mathrm{A}}\right)$ of times between synchronous events T_{A} in small-world networks $\left(N = 75 \times 75, m = 50, \rho = 0.55\right)$ of non-leaky IF oscillators ($a = 0$). Blue: $b = 0.0075$; black: $b = 0.008$; red: $b = 0.0085$. Top right: frequency distribution of event durations T_{E}. Bottom left: correlation between subsequent inter event durations T_{A}^{i} for $b = 0.008$. Bottom right: exemplary section of the time evolution of $r(t)$ for $b = 0.008$. The beginnings and endings of events were determined by threshold crossing at $\rho = 0.2$.

$b \in \left[0.006, 0.008\right]$, the networks generate periodic macroscopic dynamics, which is much slower than the frequency of single oscillators and which is an emerging property of the network that is not directly related to the oscillators' timescales (τ and ϑ). In figure 12, we show a closer inspection of the patterns that are formed during one oscillation, which are very similar to those

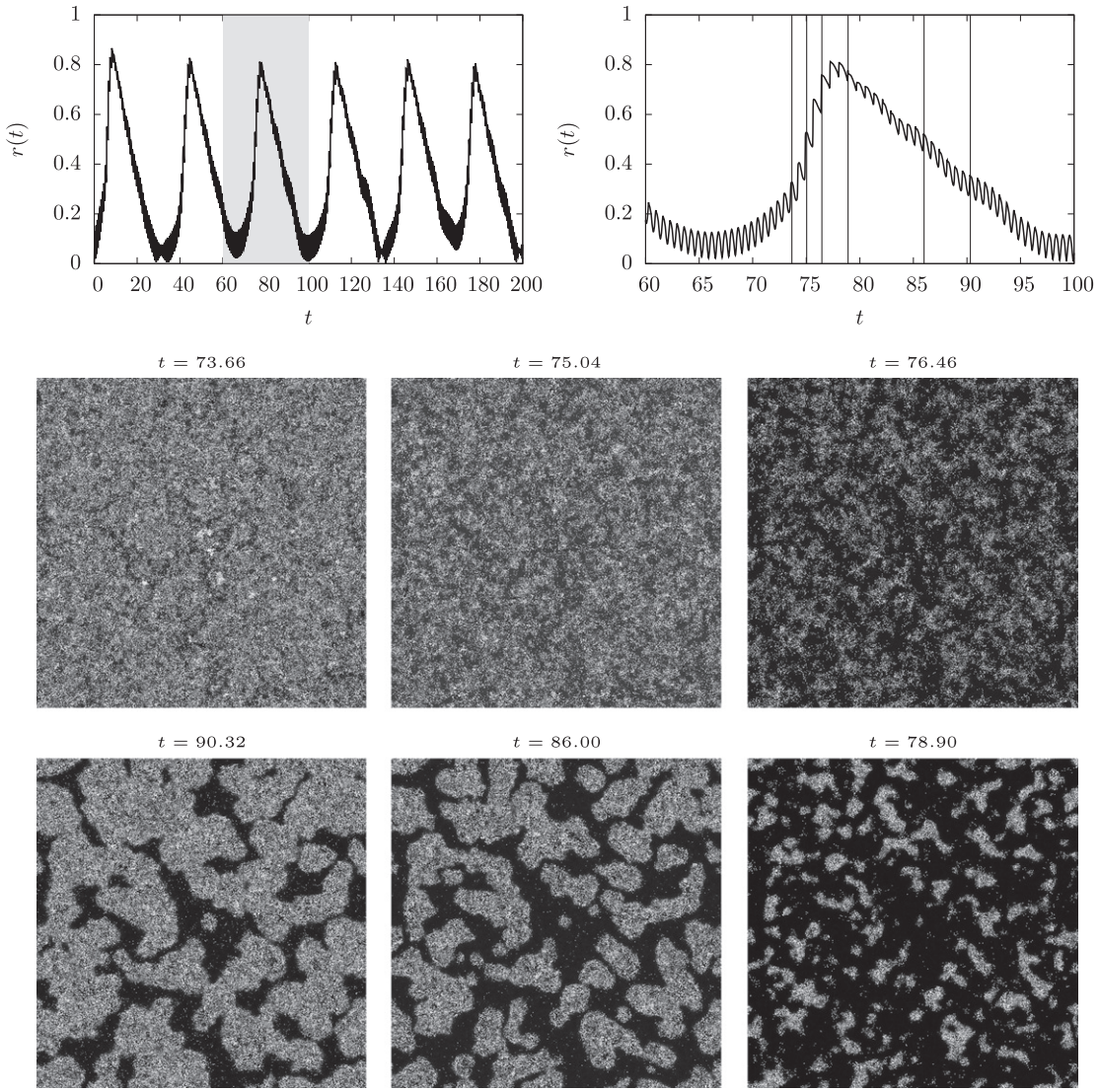

Figure 12. Top left: order parameter $r(t)$ for $\rho = 0.5$, $b = 0.008$, $N = 500 \times 500$. Bottom: snapshots of the spatial distribution of oscillator phases. Snapshots were arranged such that the ones that lie under another relate to a similar value of the order parameter r. Times of snapshots are indicated as vertical lines in the upper right plot, which shows a closer view on $r(t)$.

that can be observed during the rare events for smaller values of b. Note that a snapshot of the spatial distribution of phases represents the complete state space of the system. The time evolution is thus fully determined by the pattern, which must differ at the ascending and descending parts of events: the asynchronous part of the network is distributed at the ascending part and forms connected regions at the descending part. Synchronization may only set in once the whole network is covered by asynchronous regions. The frequency of the rhythm is determined by the size of phase responses in relation to the intrinsic dynamics. For small phase responses, patterns of arbitrary type only change over the course of many oscillations, and thus the period duration of the rhythm is large. We can shift the values of a and b that lead to oscillatory behavior to smaller

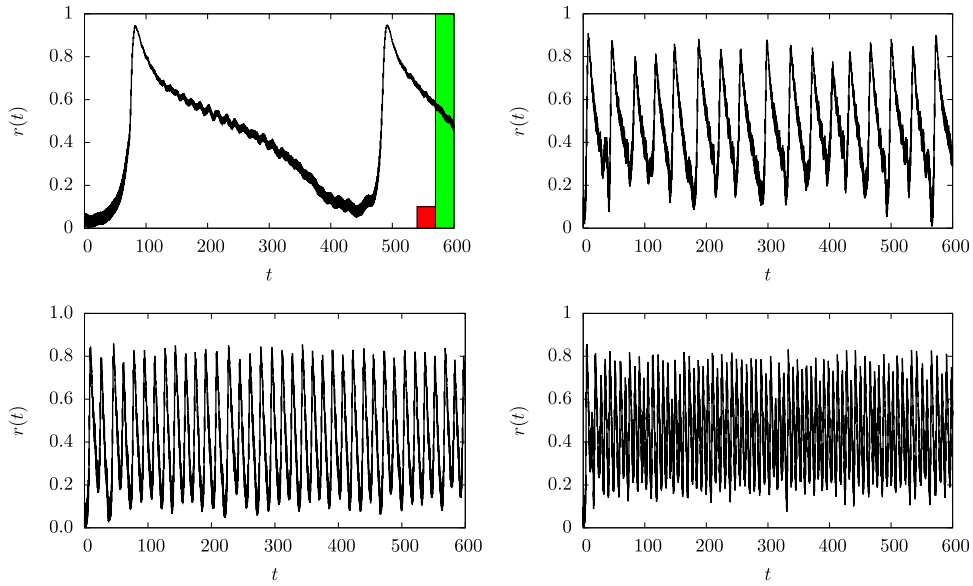

Figure 13. The time evolutions of $r(t)$ for small-world networks ($N = 250 \times 250$, $m = 50$, $\rho = 0.55$) of IF oscillators. Oscillator parameters: top left: $(a, b, \tau, \vartheta) = (0.0, 0.005, 0.02, 0.1)$; top right: $(0.0, 0.012, 0.01, 0.05)$; bottom left: $(0.0, 0.014, 0.005, 0.025)$; bottom right: $(0.0, 0.0165, 0.002, 0.01)$. The red and green bars sketch the sets S and D, respectively.

values by increasing τ and ϑ (and keeping their relation fixed). This allows us to control the frequency of the rhythm (see figure 13).

Values of $b \in [0.008, 0.012]$ lead to non-converging behavior, in which synchronization may set in even before the network is completely asynchronous. Naturally, this decreases the range of fluctuations that we observe in macroscopic observables and may lead to complicated and irregular behavior, as shown in figure 2, bottom. For $b > 0.012$, the range of fluctuations in $r(t)$ eventually vanishes, leading to constant macroscopic observables in states in which synchronization and desynchronization phenomena continuously interplay. In contrast to the chimera states, however, we here observe volatile distributions of asynchronous regions (see figure 14) that grow at boundaries and are entrained to the synchronous part from within at the same time.

6. Conclusions

Let us summarize our observations of the different macroscopic dynamics that are generated when networks split into chimera states, i.e. into spatially separated asynchronous and synchronous regions. In figure 15 we show a part of the (ρ, b)-parameter-plane with markers at the parameters that we used when describing the different dynamical behaviors. In dependence on ρ and b, the evolution of spatial patterns is determined by the growing of asynchronous regions and synchronizations of the latter via long-ranged connections. The possibility of either of these mechanisms is influenced by the amount of order in the network, i.e. the total size of the asynchronous regions in the network. We described the possibility of both mechanisms to

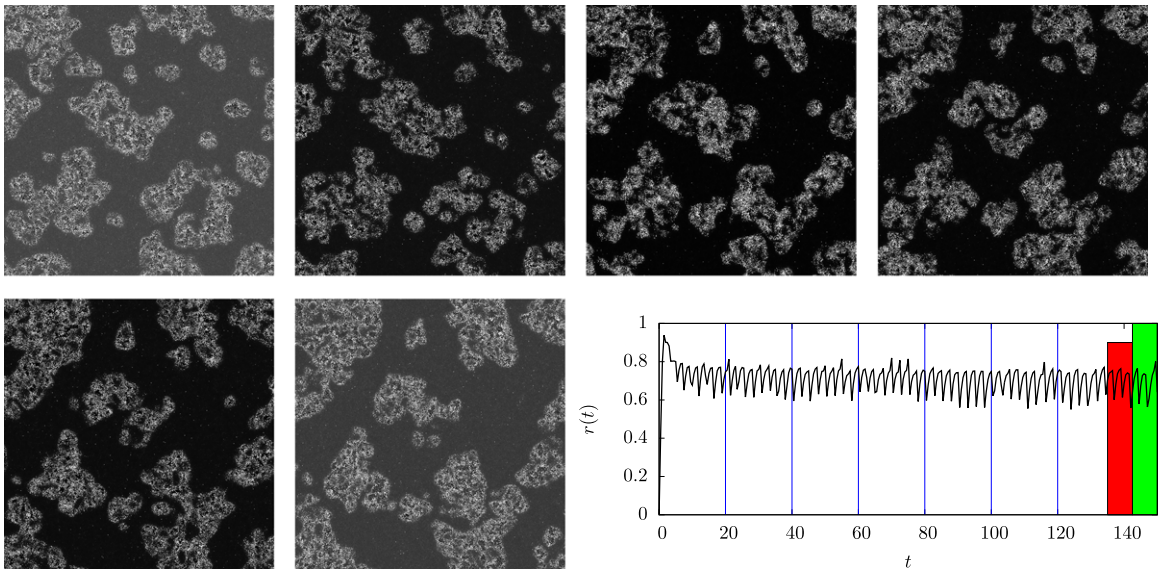

Figure 14. Snapshots of the spatial distribution of oscillator phases taken from a small-world network ($N = 500 \times 500$, $\rho = 0.5$, $m = 50$) of IF oscillators ($\tau = 0.01$, $\vartheta = 0.05$, $a = 0.008$, $b = 0.016$). Phase values range from 0 (black) to 1 (white). Times of snapshots are marked as vertical lines in the top left plot, which shows the time evolution of the order parameter $r(t)$. The networks show volatile spatial patterns in which synchronization and desynchronization phenomena facilitate an equilibrium in the size of the asynchronous pattern. The red and green bars sketch the sets S and D, respectively.

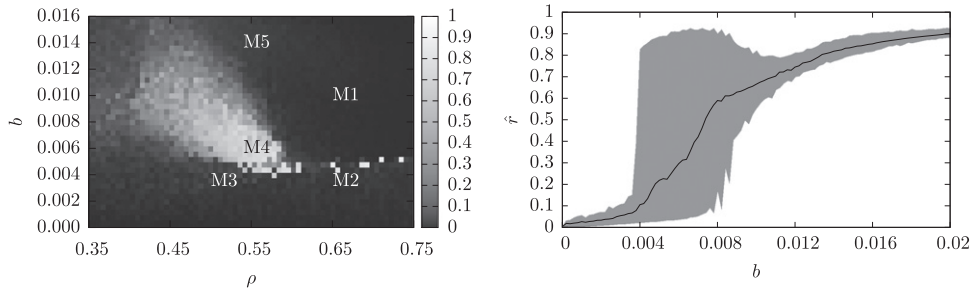

Figure 15. Left: closer view on the range $\langle \hat{r} \rangle$ of observed values of $\hat{r}$ (see figure 3) with markers indicating the control parameters ρ and b we used to describe the different dynamical behaviors. M1: chimera states (see figure 8, left); M2: chimera states and asynchronous states depending on the initial condition (see figure 8, right); M3: asynchronous states; M4: non-converging collective behavior (see figures 9–13); M5: volatile asynchronous patterns (see figure 14). Right: the smallest, largest and mean value of $\hat{r}(t)$ in $t \in [0, 5000]$ for a cut through the parameter space at $\rho = 0.55$. The dynamics shows asynchronous behavior for $b < 0.004$, recurrent events of synchronous firing for $0.004 < b < 0.006$, oscillatory behavior for $b \in [0.006, 0.008]$, irregular non-converging behavior for $0.008 < b < 0.012$, and volatile spatial patterns for $b > 0.012$.

occur by the S set of values of r for which avalanche-like synchronization may set in, and the set of D values for which the growing of asynchronous regions is possible. Graphically, this means that if r is in D, then the order parameter r will decrease as the asynchronous regions are growing. When r is in S, then r will increase rapidly during the next few oscillations due to avalanche-like synchronization. The generation of the non-converging behaviors relies on the situation where exactly one of both mechanisms is possible for a given amount of the order in the network, such that both synchronization and desynchronization alternate (M4 in figure 15). For $\rho > 0.6$, S and D do not overlap such that the growing of asynchronous regions is only possible for larger values of r and stops at some value of r that is neither in S nor in D. At this value of r, the spatial pattern is frozen into a nearly immobile chimera state (M2 and M1 of figure 15). For $b \leqslant 0.004$, synchronization is not possible even when asynchronous regions cover the whole network (M3). For b values above the region with non-converging behavior (M5), both synchronization and desynchronization are possible, leading to asynchronous regions that are growing and are synchronized from within at the same time. Finally, for small ρ and large b, the lattice structure is enforced and the networks eventually exhibit wave-like patterns. The dynamics is then no longer governed by these two distinct routes to synchrony that we described for the chimera states.

We investigated the dynamics of integrate-and-fire-like oscillators coupled onto small-world networks. Such networks represent a mixture of two well-studied organization structures —namely, random networks and regular lattices. We reported on several dynamical behaviors that uniquely rely on their dual structure and thus underline their importance for modeling of real-world phenomena, especially in the context of social or neuron networks. In random networks, we can choose parameters in such a way that both synchronous and asynchronous behavior is stable for long periods of time. However, these behaviors cannot usually be observed at the same time because random networks are too tightly knit together. In contrast, networks with a spatial dimension like the small-world networks investigated here allow for the necessary spatial separation that enables a self-organized split into synchronous regions (where oscillators share a common phase) and asynchronous regions with distributed oscillator phases that form unstructured spatial patterns. Such split states are commonly denoted as chimera states [37]. We could show that these states introduce two distinct routes to synchrony/asynchrony.

Depending on the control parameters and on the total size of the asynchronous regions, the asynchronous behavior may become unstable and be entrained to the synchronous part of the network. Similarly, the synchronous behavior may become unstable and be entrained to the asynchronous part of the network. In these cases, entrainment is mediated by long-ranged connections. Moreover, entrainment can occur at the boundaries between regions; asynchronous regions may grow or shrink, in which case entrainment is mediated by short-ranged connections. Both routes are influenced by control parameters and by the relative sizes of the synchronous and asynchronous regions in the network. For example, we identified parameters for which growing of asynchronous regions was only possible if their total size in the network was small, and asynchronous regions were only unstable when their total size was large. Depending on the possibility of (de-)synchronization via both routes, we could observe various kinds of irregular macroscopic dynamics.

Neuronal dynamics is the most obvious context for our dynamical system. In the following, we will interpret our findings accordingly. One of these irregular macroscopic dynamics took the form of recurrent events of synchrony that were embedded in extended

periods of asynchronous behavior of variable duration. From a qualitative point of view, this behavior is comparable to the dynamics seen in epilepsy patients: the standard notion is that epileptic seizures represent short periods of overly synchronous firing of a large group of neurons, while the normal functioning of the brain is usually connoted with asynchronous firing. However, the mechanisms that lead to transitions into and out of seizures are still unclear for many types of epilepsies [38, 39]. Recent computational models of epileptic brain networks usually consider noise-induced attractor switching that leads to exponentially distributed seizure and inter-seizure durations [40–43]. However, some epilepsies, especially so-called focal epilepsies, are often related to seizure times that follow a modal distribution, which possibly points to some seizure terminating mechanism [44]. The merit of our work may be to display a possible mechanism for desynchronization that persists even without inhibitory interactions and noise, and which would lead to such a modal distribution.

Another irregular macroscopic dynamic that we observed in the small-world regime was an emergent rhythm that is slower than the firing of single oscillators. By modifying the control parameters, we could control the frequency of this rhythm almost arbitrarily. The mechanism of this oscillation may improve, for example, our understanding of the generation of the respiratory rhythm. The latter is generated in a small brain region, the so-called pre-Bötzinger complex of the brain, and persists even in small slices and even when inhibition is blocked pharmacologically [45]. The generating mechanisms are still unknown but are believed to rely on the involved network structure.

Acknowledgments

We thank Gerrit Ansmann and Sebastian Werner for careful revision of an earlier version of the manuscript. This work was supported by the Deutsche Forschungsgemeinschaft (LE 660/4-2).

References

[1] Winfree A T 1967 Biological rhythms and the behavior of populations of coupled oscillators *J. Theor. Biol.* **16** 15–42
[2] Kuramoto Y 1984 Chemical oscillations waves and turbulence (Berlin: Springer Verlag)
[3] Glass L 2001 Synchronization and rhythmic processes in physiology *Nature* **410** 277–84
[4] Pikovsky A S, Rosenblum M G and Kurths J 2001 *Synchronization: A Universal Concept in Nonlinear Sciences* (Cambridge: Cambridge University Press)
[5] Arenas A, Díaz-Guilera A, Kurths J, Moreno Y and Zhou C 2008 Synchronization in complex networks *Phys. Rep.* **469** 93–153
[6] Bashan A, Bartsch R P, Kantelhardt J W, Havlin S and Ivanov P Ch 2012 Network physiology reveals relations between network topology and physiological function *Nat. Commun.* **3** 702
[7] Guevara M R and Lewis T J 1995 A minimal single-channel model for the regularity of beating in the sinoatrial node *Chaos* **5** 174–83
[8] Gonze D, Markadieu N and Goldbeter A 2008 Selection of in-phase or out-of-phase synchronization in a model based on global coupling of cells undergoing metabolic oscillations *Chaos* **18** 037127
[9] Lehnertz K, Bialonski S, Horstmann M-T, Krug D, Rothkegel A, Staniek M and Wagner T 2009 Epilepsy ed H G Schuster *Reviews of Nonlinear Dynamics and Complexity* (Berlin: Wiley-VCH) pp 159–200

[10] Varela F J, Lachaux J P, Rodriguez E and Martinerie J 2001 The brain web: Phase synchronization and large-scale integration *Nat. Rev. Neurosci.* **2** 229–39
[11] Schnitzler A and Gross J 2005 Normal and pathological oscillatory communication in the brain *Nat. Rev. Neurosci.* **6** 285–96
[12] Uhlhaas P J and Singer W 2006 Neural synchrony in brain disorders: relevance for cognitive dysfunctions and pathophysiology *Neuron* **52** 155–68
[13] Buzsáki G 2006 *Rhythms of the Brain* (New York: Oxford University Press)
[14] van Leeuwen P, Geue D, Thiel M, Cysarz D, Lange S, Romano M C, Kurths J and Groenemeyer D H 2009 Influence of paced maternal breathing on fetal-maternal heart rate coordination *Proc. Natl. Acad. Sci. USA* **106** 13661–6
[15] Bartsch R P, Schumann A Y, Kantelhardt J W, Penzel T and Ivanov P Ch 2012 Phase transitions in physiologic coupling *Proc. Natl. Acad. Sci. USA* **109** 10181–6
[16] Kuramoto Y and Battogtokh D 2002 Coexistence of coherence and incoherence in nonlocally coupled phase oscillators *Nonlinear Phenom. Complex Syst.* **5** 380–5
[17] Abrams D M and Strogatz S H 2004 Chimera states for coupled oscillators *Phys. Rev. Lett.* **93** 174102
[18] Abrams D M, Mirollo R, Strogatz S H and Wiley D A 2008 Solvable model for chimera states of coupled oscillators *Phys. Rev. Lett.* **101** 084103
[19] Omel'chenko O E, Maistrenko Y L and Tass P A 2008 Chimera states: The natural link between coherence and incoherence *Phys. Rev. Lett.* **100** 044105
[20] Laing C R 2009 Chimera states in heterogeneous networks *Chaos* **19** 013113
[21] Sheeba J H, Chandrasekar V K and Lakshmanan M 2009 Globally clustered chimera states in delay-coupled populations *Phys. Rev.* E **79** 055203(R)
[22] Wolfrum M and Omelchenko E 2011 Chimera states are chaotic transients *Phys. Rev.* E **84** 015201
[23] Laing C R, Rajendran K and Kevrekidis I G 2012 Chimeras in random non-complete networks of phase oscillators *Chaos* **22** 013132
[24] Wildie M and Shanahan M 2012 Metastability and chimera states in modular delay and pulse-coupled oscillator networks *Chaos* **22** 043131
[25] Rothkegel A and Lehnertz K 2011 Recurrent events of synchrony in complex networks of pulse-coupled oscillators *Europhys. Lett.* **95** 38001
[26] Burkitt A N 2006 A review of the integrate-and-fire neuron model: I Homogeneous synaptic input *Biol. Cybern.* **95** 1–19
[27] Mirollo R E and Strogatz S H 1990 Synchronization of pulse-coupled biological oscillators *SIAM J. Appl. Math.* **50** 1645–62
[28] Watts D J and Strogatz S H 1998 Collective dynamics of 'small-world' networks *Nature* **393** 440–2
[29] Meron E 1992 Pattern formation in excitable media *Phys. Rep.* **218** 1–66
[30] Arenas A, Díaz-Guilera A and Perez-Vicente C J 2006 Synchronization reveals topological scales in complex networks *Phys. Rev. Lett.* **96** 114102
[31] Barthélemy M 2011 Spatial networks *Phys. Rep.* **499** 1–101
[32] Rothkegel A and Lehnertz K 2012 Conedy: A scientific tool to investigate complex network dynamics *Chaos* **22** 013125
[33] Rothkegel A and Lehnertz K 2009 Multistability, local pattern formation, and global collective firing in a small-world network of non-leaky integrate-and-fire neurons *Chaos* **19** 015109
[34] Tel T and Lai Y C 2008 Chaotic transients in spatially extended systems *Phys. Rep.* **460** 245–75
[35] Zumdieck A, Timme M, Geisel T and Wolf F 2004 Long chaotic transients in complex networks *Phys. Rev. Lett.* **93** 244103
[36] Zou H-L, Li M, Lai C-H and Lai Y-C 2012 Origin of chaotic transients in excitatory pulse-coupled networks *Phys. Rev.* E **86** 066214
[37] Tinsley M R, Nkomo S and Showalter K 2012 Chimera and phase-cluster states in populations of coupled chemical oscillators *Nat. Phys.* **8** 662–5

[38] Lytton W W 2008 Computer modelling of epilepsy *Nat. Rev. Neurosci.* **9** 626–37
[39] Mormann F, Andrzejak R, Elger C E and Lehnertz K 2007 Seizure prediction: the long and winding road *Brain* **130** 314–33
[40] Lopes da Silva F H, Blanes W, Kalitzin S N, Parra J, Suffczynski P and Velis D N 2003 Dynamical diseases of brain systems: different routes to epileptic seizures *Biomedical Engineering, IEEE Transactions on* **50** 540–8
[41] Takeshita D, Sato Y D and Bahar S 2007 Transitions between multistable states as a model of epileptic seizure dynamics *Phys. Rev.* E **75** 051925
[42] Suffczynski P, Lopes da Silva F H, Parra J, Velis D and Kalitzin S 2005 Epileptic transitions: Model predictions and experimental validation *J. Clin. Neurophysiol.* **22** 288–99
[43] Suffczynski P, Wendling F, Bellanger J J and Lopes Da Silva F H 2006 Some insights into computational models of (patho)physiological brain activity *Proc. IEEE* **94** 784–804
[44] Lado F A and Moshé S L 2008 How do seizures stop? *Epilepsia* **49** 1651–64
[45] Feldman J L and Del Negro C A 2006 Looking for inspiration: new perspectives on respiratory rhythm *Nat. Rev. Neurosci.* **7** 232–42